Reusable and long-lasting active micro-cleaners for heterogeneous water remediation

Jemish Parmar[1, 2±], Dr. Diana Vilela[1±], Dr. Eva Pellicer[3], Dr. Daniel Esqué-de los Ojos[4], Prof. Dr. Jordi Sort[3, 5] and Prof. Dr. Samuel Sánchez[1, 2,5]

1. Max-Planck Institute for Intelligent Systems, Heisenbergstr. 3, 70569 Stuttgart, Germany. E-mail: sanchez@is.mpg.de;

2. Institute for Bioengineering of Catalonia (IBEC), Baldiri I Reixac 10-12, 08028 Barcelona, Spain. E-mail: ssanchez@ibecbarcelona.eu

3. Departament de Física, Universitat Autònoma de Barcelona, 08193, Bellaterra, Spain

4. The School of Materials, The University of Manchester, Oxford Road, Manchester, M13 9PL, UK

5. Institució Catalana de Recerca i Estudis Avançats (ICREA), Psg. Lluís Companys, 23, 08010 Barcelona, Spain

±These authors contributed equally to this work.

Keywords: Micro-cleaners, catalytic micro motors, Nano-robots, wastewater treatment, heterogeneous catalyst

Self-powered micro-machines are promising tools for the future environmental remediation technology. Waste water treatment and water reuse is an essential part of environmental sustainability. Herein, we present reusable Fe/Pt multi-functional active micro-cleaners that are capable of degrading organic pollutants by generated hydroxyl radicals via Fenton-like reaction. Various different properties of micro-cleaners such as the effect of their size, short-term storage, long-term storage, reusability, continuous swimming capability, surface composition and mechanical properties are studied. We find that micro-cleaners can

continuously swim for more than 24 hours and can be stored more than 5 weeks during multiple cleaning cycles. Micro-cleaners can also be reused, which reduces the cost of the process. Over the reuse cycles, the outer iron surface of the Fe/Pt micro-cleaners generates *in-situ* heterogeneous Fenton catalyst and releases a low concentration of iron into the treated water while the mechanical properties also appear to be improved due to both surface composition and structural changes. Results have been characterized by SEM, XPS, Nanoindentation and Finite Element Modeling (FEM).

1. Introduction

It has long been known that organic and industrial wastewater poses a serious threat to the environment and if the wastewater is released untreated, it can damage aquatic life and is harmful to human health[1–3]. Since the last century, significant efforts have been made to improve the efficiency of water treatment methods[4–8]. However, due to the increasing population and pollution, water cleaning is becoming increasingly challenging[9–11]. With the advancement of nanotechnology, new catalysts and engineered nanomaterials are being developed for water treatment[12–14]. One of the growing areas in nanotechnology is micro and nano-robots or motors, envisioned to carry out complex medical tasks such as drug delivery, cancer treatment and microsurgery[15–18]. Catalytic self-propelled micro-motors use chemical fuel such as hydrogen peroxide, hydrazine[19] or acetylene[20] for propulsion. Amongst them, hydrogen peroxide is being most widely used as a fuel in combination with the platinum catalyst for propulsion[21]. However, due to the highly oxidative nature of hydrogen peroxide, medical applications of micromotors are limited at their current state[22,23]. Nonetheless, environmental applications of motors have shown promising results[24,25]. Recent advances in this area demonstrated degradation of organics[26–29] and chemical warfare agent[30–32], sensing

of heavy metal[33], separation of organic materials[34] and oil removal[35] capabilities of nano/micromotors.

Iron-containing micromotors swimming in hydrogen peroxide serve as micro-cleaners to degrade organic pollutants *via* Fenton-like reaction[26]. The degradation rate of organics is much higher when motile micro-cleaners are deployed compared to degradation using non-motile iron-containing tubes. Hydrogen peroxide is the main reagent in Fenton reaction, which is already in use for many commercial water treatment procedures[36]. Hydrogen peroxide is also considered as a green reagent for sustainable chemistry because it can be degraded into water and oxygen gas without producing any toxic chemicals[37,38]. The classical Fenton reaction generates hydroxyl radicals when Fe^{2+} reacts with hydrogen peroxide, as follows[36,39–42]:

$$Fe^{2+} + H_2O_2 \rightarrow Fe^{3+} + OH^{\bullet} + OH^{-} \qquad (1)$$

$$Fe^{3+} + H_2O_2 \rightarrow Fe^{2+} + HO_2^{\bullet} + H^{+} \qquad (2)$$

During the reaction chain, Fe^{2+} oxidizes to Fe^{3+} and Fe^{2+} regenerates back from Fe^{3+}(equations 1 and 2). One of the main disadvantages of the classical Fenton reaction is that at the end of the treatment iron ions need to be removed from the solution. Iron salt removal requires a high amount of chemicals for precipitation and produces a large amount of sludge. Further sludge removal is an expensive process and requires a lot of energy. In addition, non-reusability of iron salt as a catalyst and energy requirement for mixing results in extra cost for the treatment. To overcome the disadvantages of classical homogeneous Fenton reaction, significant efforts have been made to develop heterogeneous Fenton catalysts[43].

Towards the development of more practical use of micro-cleaners and to overcome the limitation of Fenton reaction, we developed micro-cleaners that can be reused several times

for batch cleaning, can swim continuously for hours and can be stored for weeks for later use, also minimizing the iron release to the solution by generating in-situ heterogeneous catalyst from iron surface. The effect of different micro-cleaner sizes on the organic dye degradation rate, chemical composition after the cleaning cycles and mechanical properties of micro-cleaners were studied to understand the system thoroughly. We extended the applicability of micro-cleaners to another model of organic contaminant, i.e. 4-nitrophenol, demonstrating their versatile remediation functionalities.

2. Results and discussion

2.1. Size effect of micro-cleaners on dye degradation and reusability

Pre-strained nanomembranes of iron and platinum were sequentially evaporated by e-beam on photoresist squared patterns of different sizes. The nanomembranes were selectively lifted off from the glass substrate and rolled up into micro tubular structures (Movie S1), leading to the formation of the micro-cleaners as explained in the experimental section. We studied the effect of size of the Fe/Pt micro-cleaners on the degradation rate using three different sizes of micro-cleaners. For all sizes, we deposited equal area of previously designed photoresist patterns to keep the amount of catalytic material the same in each experiment even though the total number of tubes was different. Three sizes of micro-cleaners (200 µm, 300 µm and 500 µm long) were fabricated by rolling up Fe/Pt nanomembranes **(Figure 1A and Figure 1B)** and used for the degradation of dye. Experimental parameters for the dye degradation are presented in the experimental section.
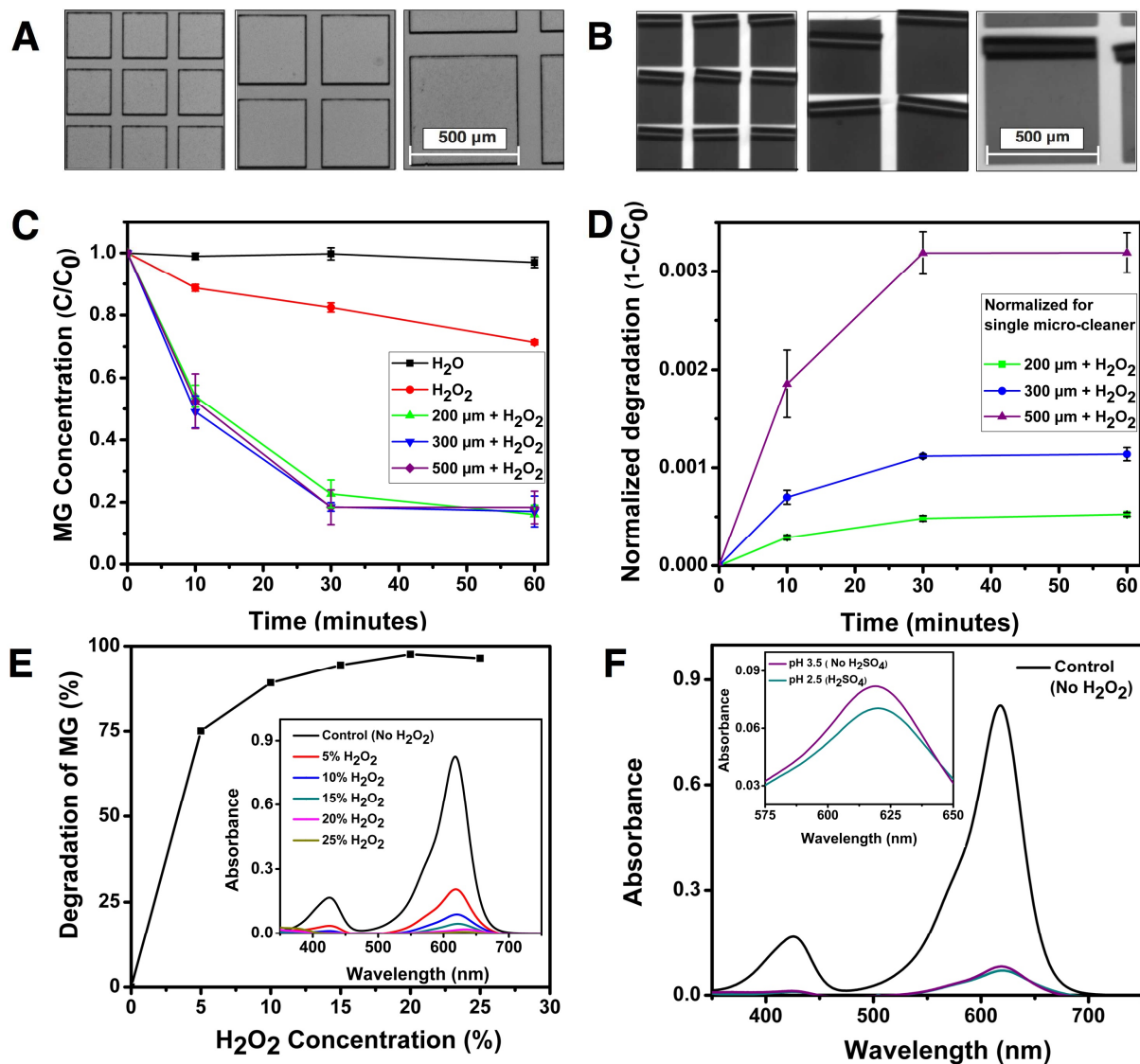
Figure 1. Fabrication of micro-cleaners and their use in the degradation of malachite green (MG) dye. (A) 200 µm, 300 µm and 500 µm square photoresist patterns with e-beam evaporated Fe/Pt nanomembranes on it. (B) Fe/Pt nanomembranes rolled up into 200 µm, 300 µm and 500 µm long micro-cleaners with approximate diameter of 40 to 60 µm. (C) Degradation of dye over the time using different sizes of micro-cleaners. (D) Dye degradation over time normalized for single micro-cleaners of different sizes. (E) Degradation of malachite green at different concentrations of hydrogen peroxide by 500 µm micro-cleaners in 60 minutes (insert shows the light absorbance spectrum of malachite green at different concentration). (F) Degradation of malachite green in 60 minutes, with and without the addition of H_2SO_4

5

Classical Fenton reaction is highly oxidative in nature because of the hydroxyl radical production during the reaction of Fe^{2+} ions with hydrogen peroxide that are capable of completely oxidizing organic molecules. Degradation of a model pollutant dye malachite green via classical Fenton reaction was studied in detail using iron salt (ferrous sulfate) as the source of Fe^{2+} ions[44]. However, external mixing used during the degradation reaction and removal of sludge produced by Fe^{2+} ions *via* precipitation after the completion of the reaction can make the process expensive. In similar experimental conditions, active micro-cleaners showed similar results but without any external mixing and less amount of iron released from the surface into the treated water. Micro-cleaners act as multipurpose agents, the platinum layers present inside the micro-cleaner act as the engine to decompose H_2O_2 into O_2 and H_2O. The oxygen bubble trail produces thrust on the micro-cleaner to propel it which additionally provide micro mixing and enhanced mass transfer[45–47]. The iron layer present outside the micro-cleaners reacts with the H_2O_2 to produce hydroxyl radicals via Fenton-like reaction that degrades the organic compound. The pH was adjusted to 2.5 using sulfuric acid (the reported optimum pH is between 2-3 for the Fenton reaction catalyzed by zero valent metallic iron[48,49]) and the initial concentration of malachite green was kept to 50 µg/ml in all the experiments. During the dye degradation experiments, dye concentration was periodically measured by the UV-visible spectrometer and the micro-cleaners were left swimming in the contaminated dye solution until steady state of degradation was observed after 60 minutes. **Figure 1C** shows the degradation curves of 200 µm, 300 µm, and 500 µm micro-cleaners and control experiments without micro-cleaners. Micro-cleaners degraded more than 80 % of malachite green in 60 minutes; furthermore, complete degradation can be achieved over longer time (not shown). After 60 minutes of degradation, we measured the degradation of malachite green for all the three sizes of micro-cleaners. We calculated one-way analysis of variance (ANOVA) for all measured data points for different sizes of micro-cleaners to verify

the statistically significant difference between them. There was no significant difference found in the amount of dye degraded by the three different sizes of micro-cleaners at the P = 0.9850 (n=5) level. Degradation of malachite green dye is due to the oxidation reaction facilitated by hydroxyl radicals produced while the iron containing micro-cleaners are swimming in wastewater containing hydrogen peroxide. Hydroxyl radicals have very strong oxidation potential (2.8 V) just below the oxidation potential of fluorine (3V); therefore, if enough time is given, hydroxyl radicals can mineralize organic molecules into carbon dioxide without leaving any toxic byproducts. Hydroxyl radicals oxidize malachite green into final byproduct oxalic acid before mineralizing into carbon dioxide [50].

Clearly, Fe/Pt micro-cleaners show higher degradation rate compared to the control experiments without the micro-cleaners as **Figure 1C** shows. Fe/Pt micro-cleaners were already shown to outperform the dye degradation rate compared to various controls such as: (a) only Fe tubes, (b) non-iron containing motors, i.e, Ti/Pt and (c) immobilized Fe/Pt micro-cleaners[26]. **Figure 1D** show dye degradation by a single micro-cleaner considering that all micro-cleaners present in the solution contribute equally to the total degradation. The figure reveals that a larger micro-cleaner of 500 µm is more effective than a 300 µm or a 200 µm micro-cleaner. Provided that the amount of total rolled up catalytic material present in the solution is equal, i.e. 0.64 cm^2 in all cases, differences in the size of micro-cleaners do not give added advantage and have limited effect on the degradation of dye in the studied size range. The total amount of catalytic material plays a more important role than the size of the micro-cleaners. Different experimental parameters such as the effect of hydrogen peroxide concentration and the addition of H_2SO_4 were further studied by using 500 µm micro-cleaners fabricated in a new batch. **Figure 1E** shows the percentage of degradation of 50 µg/ml malachite green by micro-cleaners in 60 minutes at the different concentrations of hydrogen peroxide. Above 15 % hydrogen peroxide, the degradation percentage does not increase

significantly, reaching a plateau. **Figure 1F** shows the absorbance spectrum of malachite green after 60 minutes of degradation by micro-cleaners with and without the addition of sulfuric acid for 2.5 pH maintenance. Interestingly, the effect of sulfuric acid addition on the degradation percentage is almost negligible, meaning that in future applications, addition of acidic media is not required for the degradation of organics using micro-cleaners.
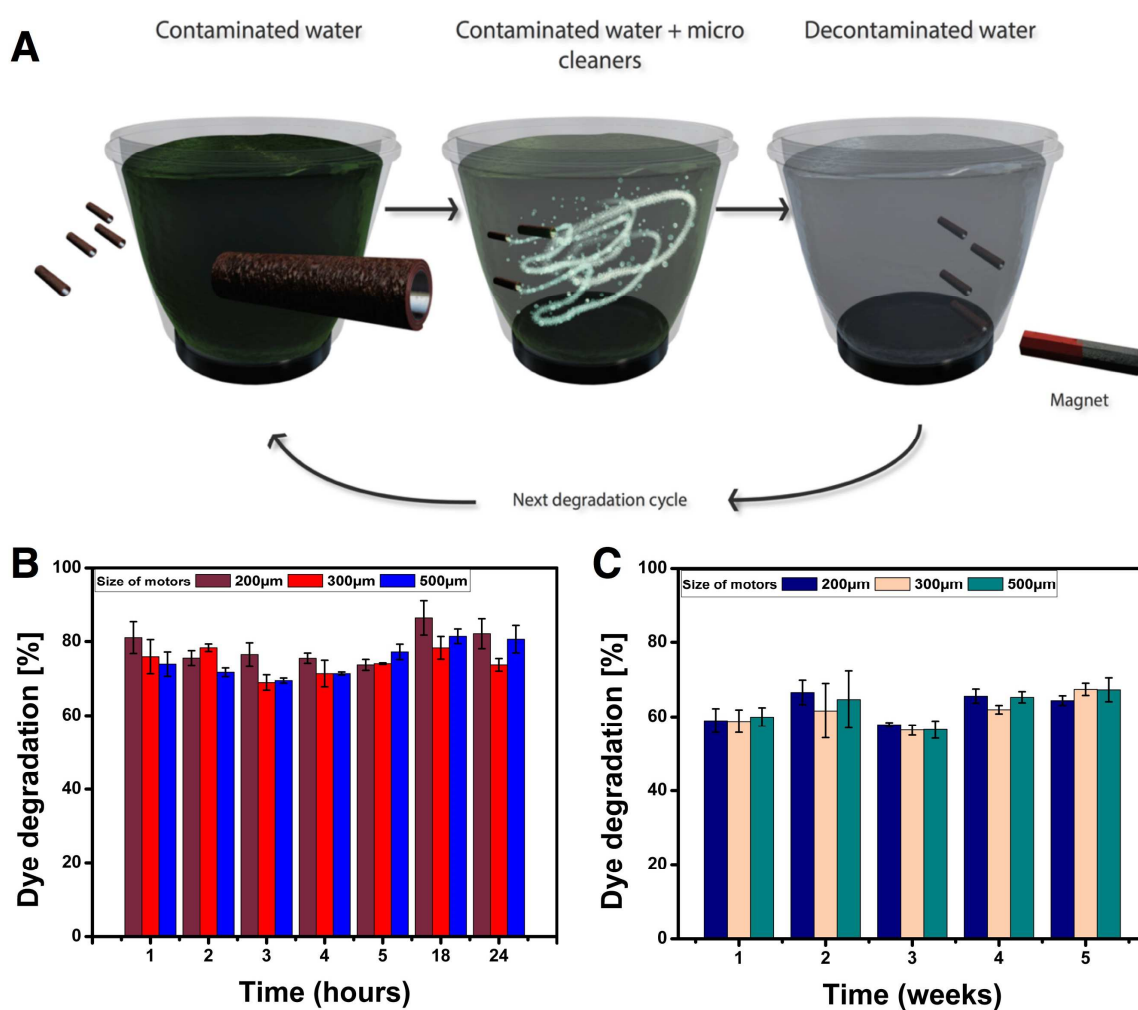

Figure 2. Reusability of micro-cleaners (A) Schematic diagram of reusability cycle of micro-cleaners. Ferromagnetic micro-cleaners were collected with an external magnet. After cleaning the surfaces of the micro-cleaners, new dye-contaminated water was added for the next degradation cycle. (B) Reusability performance of different sizes of micro-cleaners in 5 consecutive degradations during periods from 1 to 5 hours and at 18 hours and 24 hours after short-term storage. One degradation cycle is 60 minutes of swimming of micro-cleaners in

polluted water. (C) Reusability performance of micro-cleaners in each cycle after 1 to 5 weeks of storage

A reusable catalyst is important for cost effectiveness of the Fenton-based advanced oxidative processes. The reusability performance of micro-cleaners was studied as shown in **Figure 2A.** We tested all three sizes of micro-cleaners for reusability to verify if the performance remains comparable in later cycles. In each cleaning cycle, we kept the micro-cleaners swimming in the malachite dye contaminated water for the degradation. After each cleaning cycle, the micro-cleaners were collected using a permanent magnet, cleaned with ultrapure water three times and then reused in subsequent cleaning cycles. The time intervals between two cycles were chosen in incremental fashion in order to capture both short-term or long-term changes and the effect on the degradation rate. The first five cleaning cycles were performed consecutively from 1 to 5 hours, then next cycles were performed after 18 hours and 24 hours of storage in sodium dodecyl sulfate (SDS) containing water solution without hydrogen peroxide to study changes after short term storage. Following cycles were performed while keeping 1-week time interval between each cycle.

Degradation of the dye from 1 to 5 hours, when micro-cleaners were reused continuously without storing them and at 18 hours and 24 hours after short-term storage was between 68%-86%, as shown in the **Figure 2B**. After long-term storage (one week to five weeks), the degradation was slightly reduced to 56%-67%, as presented in **Figure 2C**. Percentages of degradation are in the similar range for different sizes of micro-cleaners in the different dye degradation cycles in short-term and long-term uses, which shows that the size of micro-cleaners remains unimportant in terms of reusability.

Previously, iron layers were used for magnetic steering and guiding purpose[51]. Here, we exploited the ferromagnetic nature of the Fe layer as an added functionality to recover micro-

cleaners, along with Fenton reaction capability. Micro-cleaners can be magnetically recovered and reused several times without significant changes in the percentage of dye degradation efficiency, even after weeks of storage.

After each reusability cycle, the swimming behavior of the micro-cleaners was observed under an optical microscope to assess the motility and bubble production activity. We observed that from second cycle onwards the micro-cleaners were producing bubbles more vigorously because of the self-cleaning and activation of platinum surface in the first cycle. Micro-cleaners remained active after 5 weeks (including both short-term and long-term intermediate storage, see Movie S5). Micro-cleaners presented very good structural integrity during initial cycles but in the later cycles, some longer micro-cleaners were broken into two pieces or broken layers were visible while some shorter micro-cleaners were broken in even smaller pieces without tubular geometry. Damage in the structure could be due to (i) multiples exposure of micro-cleaners to the external magnetic field of a strong neodymium-iron-boron magnet during recovery process after every cycle and (ii) internal pressure of bubbles generated while swimming. Damage in the structural integrity could be one of the reasons for the observed decrease of dye degradation percentage in the later cycles after long-term storage **(Figure 2C).**
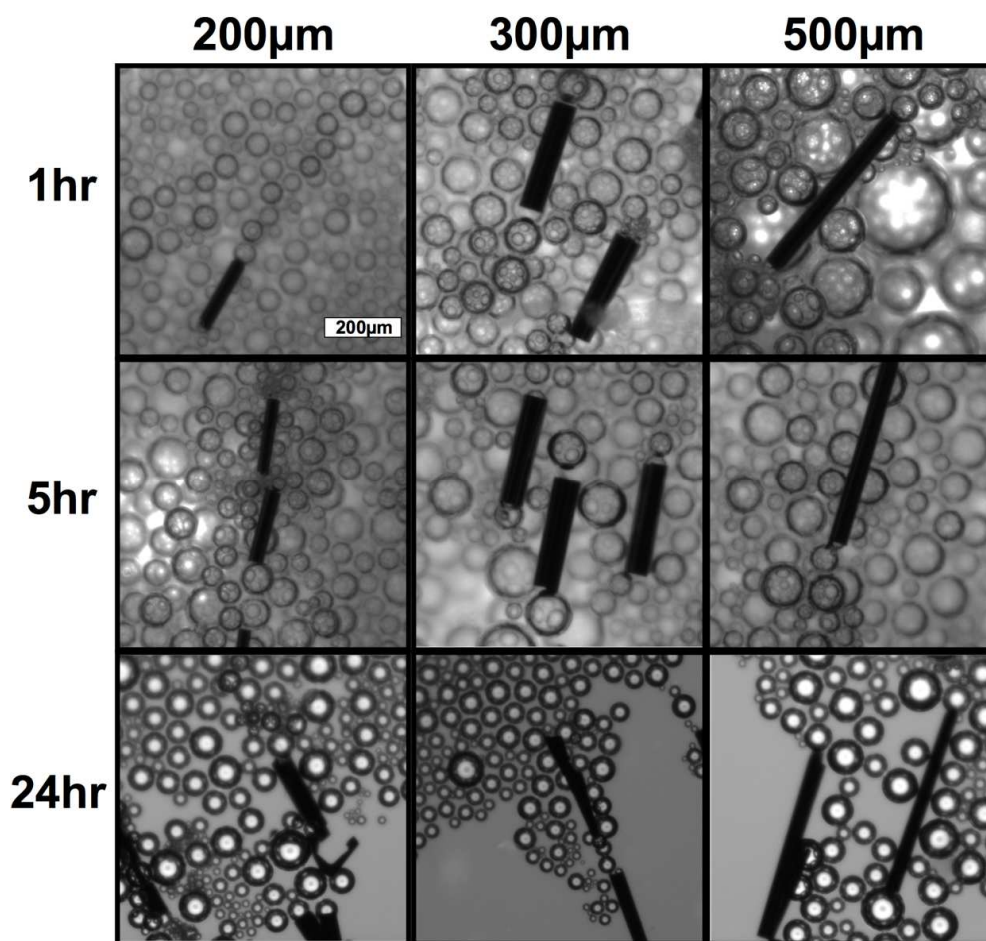
Figure 3. Micro-cleaners of three different sizes (200 µm, 300 µm and 500 µm long) swimming continuously at time intervals of 1 hour, 5 hours and 24 hours.

We carried out a separate continuous swimming experiment to understand if it is possible to use micro-cleaners for continuous longer swimming applications or many batch-wise shorter cleaning cycles. All three sizes of micro-cleaners swam in H_2O_2 (15% v/v) solution for 24 hours and swimming was periodically monitored under optical microscope (Movie S2 to S4). **Figure 3** shows that all 200 µm, 300 µm and 500 µm micro-cleaners swam even after 24 hours of continuous motion. Thus, it is indeed possible to use them for long-term swimming activity. Although some micro-cleaners were broken into smaller pieces after few hours of swimming, they were still active. Changes in the diameter were also observed after few hours of swimming as in **Figure 3**. Namely, a decrease in the diameter is visible for longer micro-

11

cleaners in 24 hours images. An opposite effect was observed for 200 µm micro-cleaners; some of them were opened up and broken into pieces. This difference is due to the presence of fewer numbers of windings in the micro-cleaners fabricated from the smaller photoresist patterns. Since the same thickness of Fe/Pt nanomembranes rolled up from different sizes of photoresist patterns, similar diameters between 40 to 60 µm (and thus, different number of windings in the rolled up tubular micro-cleaner structure) were achieved.

2.2 **Heterogeneous catalytic shift in the Fenton reaction and surface characterization**

It is widely accepted that zero valent iron-mediated Fenton reaction is mainly a manifestation of ferrous ions generated from the iron surface in acidic pH. Fe^{2+} ions leached from the surface in the solution play an important role in the reaction kinetics, which oxidizes into Fe^{3+} ions during the Fenton reaction (equation 1). Regeneration rate of Fe^{2+} ions from Fe^{3+} (equation 2) is a rate-limiting factor for classical Fenton reaction and the presence of metallic surface are believed to help the reduction of Fe^{3+} ion to Fe^{2+}, thus maintaining the Fenton reaction rate[49].

The iron released from the surface of micro-cleaners in the solution was measured by inductively coupled plasma spectrometry (ICP-OES). Measurements were performed after 60 minutes of degradation cycle for up to 8 cycles. The measured iron concentrations for all three sizes of micro-cleaners 200 µm, 300 µm and 500 µm after the first cleaning cycle are ca. 2.10, 2.15 and 2.20 µg/ml respectively. The similar concentration of iron in the solution for all sizes (**Figure 4A**) further proves a similar initial dye degradation rate for different sizes of motors (**Figure 1C**). In the subsequent cycles, the concentration dropped sharply, and remained in a lower range, as shown in **Figure 4A**.

The initial ferrous ion concentration in the reaction mixture greatly affects the kinetics of the Fenton reaction. As reported by Hameed et al., an iron concentration above 2 µg/ml is sufficient to carry out classical homogeneous Fenton degradation of malachite green.[44] However, if the Fe^{2+} concentration in the solution is below 1 µg/ml, the malachite green degradation rate should not be higher than the rate observed in the control experiment without Fe^{2+}. The dye degradation in first cycle can be attributed to the released iron from the surface of micro-cleaners but from the second cycle onwards, the iron concentration was below 1 µg/ml. In spite of having the iron concentration lower than 1 µg/ml, percentage of degradation only changes marginally. This result suggests a shift of the reaction pathway towards the heterogeneous Fenton reaction. There should be the formation of in-situ heterogeneous Fenton catalyst on the surface of the micro-cleaners to achieve a dye degradation efficacy as in the first cycle. Also, the motion of micro-cleaners can keep regenerating the active surfaces and increases the mass transfer to help maintaining the percentage of dye degradation.
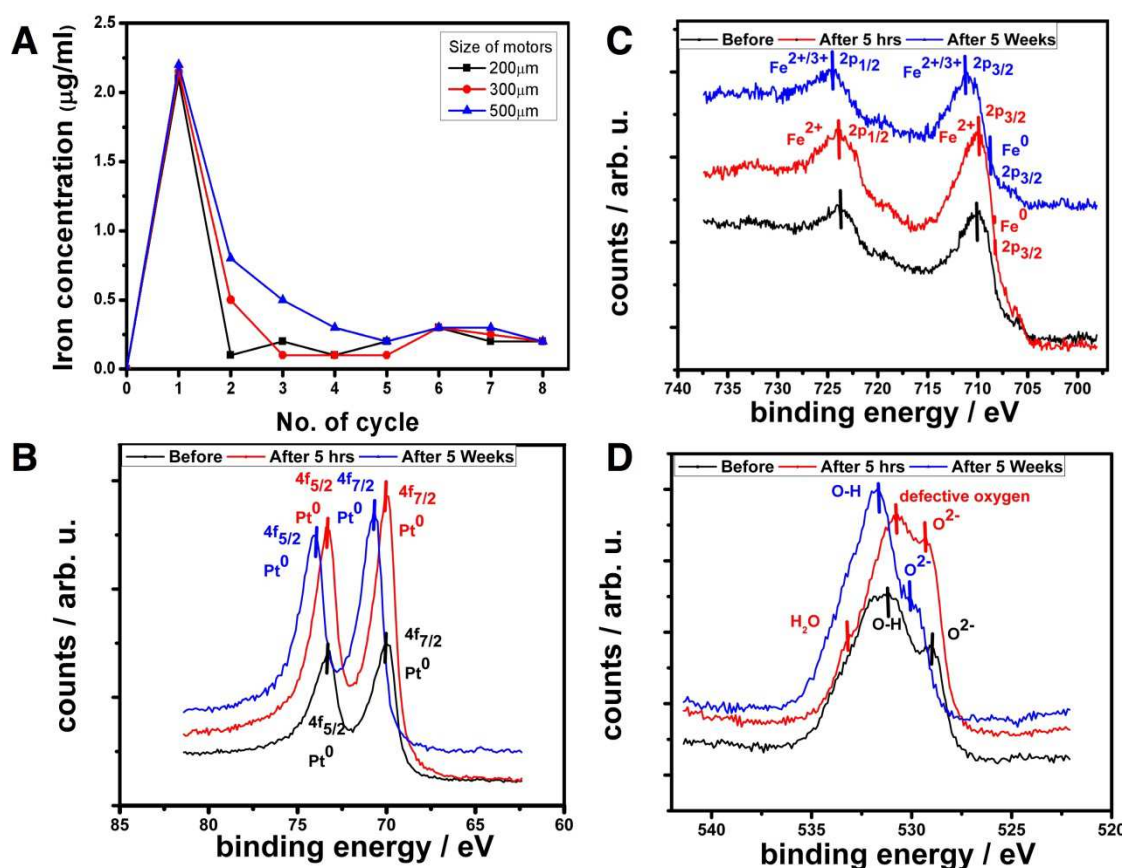

13

Figure 4. Iron release in the solution and the surface characterization of micro-cleaners. (A) Iron concentration released in the solution after first cleaning cycle was above 2µg/ml, which decreased rapidly in the consecutive cycles and remained extremely low. (B, C, D) Fe 2p, Pt 4f and O 1s high resolution XPS spectra on the surface of micro-cleaners before Fenton reaction after 5 hours of consecutive cleaning cycles and in the cycle after term storage of 5 weeks.

To study surface changes occurred after Fenton reactions, micro-cleaners were analyzed by X-ray photoelectron spectroscopy (XPS) using a PHI 5500 multi-technique system spectrometer, equipped with a monochromatic X-ray source. The micro-cleaners before Fenton reaction, after Fenton reaction of 5 hours and after 5 weeks of storage were subjected to XPS analysis. The micro-cleaners were washed with water and then dried in an ethanol-CO_2 critical point dryer before measurements (to dry without damaging the structure). Critical point drying is necessary to avoid the mechanical stresses generated due to the surface tension changes when the solvent on and around the micro-cleaners is drying.

Fe is mostly present in an oxidized form at the outermost surface already before the Fenton reaction, as evidenced by the existence of a Fe2p doublet located at 709.8 and 723.9 eV, which can be assigned to Fe^{2+} [52,53] **(Figure 4C).** It is plausible to assume that the *in situ* generation of Fe_xO_y heterogeneous catalyst[43] at the surface of the micro-cleaners reacts with hydrogen peroxide to yield reactive oxidative species in the Fenton-like reaction after first use. In fact, the Fe 2p doublet is slightly shifted toward higher binding energies after 5 weeks of storage, indicating the presence of Fe^{3+}. According to the literature, peak positions shift toward higher binding energies as the oxidation state of Fe increases[54]. Although the difference in binding energy between Fe^{2+} and Fe^{3+} oxidation states is very small (therefore, it is difficult to determine the relative amount of Fe^{2+} and Fe^{3+} in the micro-cleaners), it is clear that the surface becomes more oxidized. Notice also that the shoulder observed ca. 706 eV

14

both before and after 5 hours of Fenton reaction and attributed to metallic Fe $(2p_{3/2})$[55] weakens after 5 weeks. Hence, a complex mixture of iron oxides (FeOOH, Fe_3O_4 or Fe_2O_3) is probably present at the surface of the micro-cleaners after 5 weeks. Also, a slight shift in Pt 4f doublet is observed after 5 weeks of Fenton **(Figure 4B).** This might indicate oxidation of metallic Pt, but to a much less extent than Fe owing to the noble nature of Pt. Regarding the O 1s core-level spectra, a complex, broad signal with several maxima is observed **(Figure 4B).** After 5 hours of Fenton reaction the contribution from lattice O^{2-} (529 eV) relatively increases, indicating again that the surface is more oxidized. Likewise, the peak at 530.7 eV has been attributed to non-stoichiometric oxides in the surface region (oxygen deficiencies)[56]. After 5 weeks, the O1s signal is dominated by the contributions from hydroxyl groups. Moreover, the Fe/Pt ratio markedly diminishes after Fenton reaction: 1.51 before Fenton; 1.37 after Fenton for 1 h; 0.90 after Fenton for 5 weeks, indicating that Fe undergoes leaching, in agreement with ICP analyses.

2.3 Mechanical behaviour of Fe/Pt micro-cleaners

In order to assess the mechanical robustness and integrity of the micro-cleaners, nanoindentation experiments were performed on the rolled tubular micro-cleaners obtained from the 500 × 500 μm Fe/Pt flat films. Experiments were carried out (i) before Fenton reaction (ii) after 5 hours of Fenton reaction and (iii) after 5 weeks of storage.
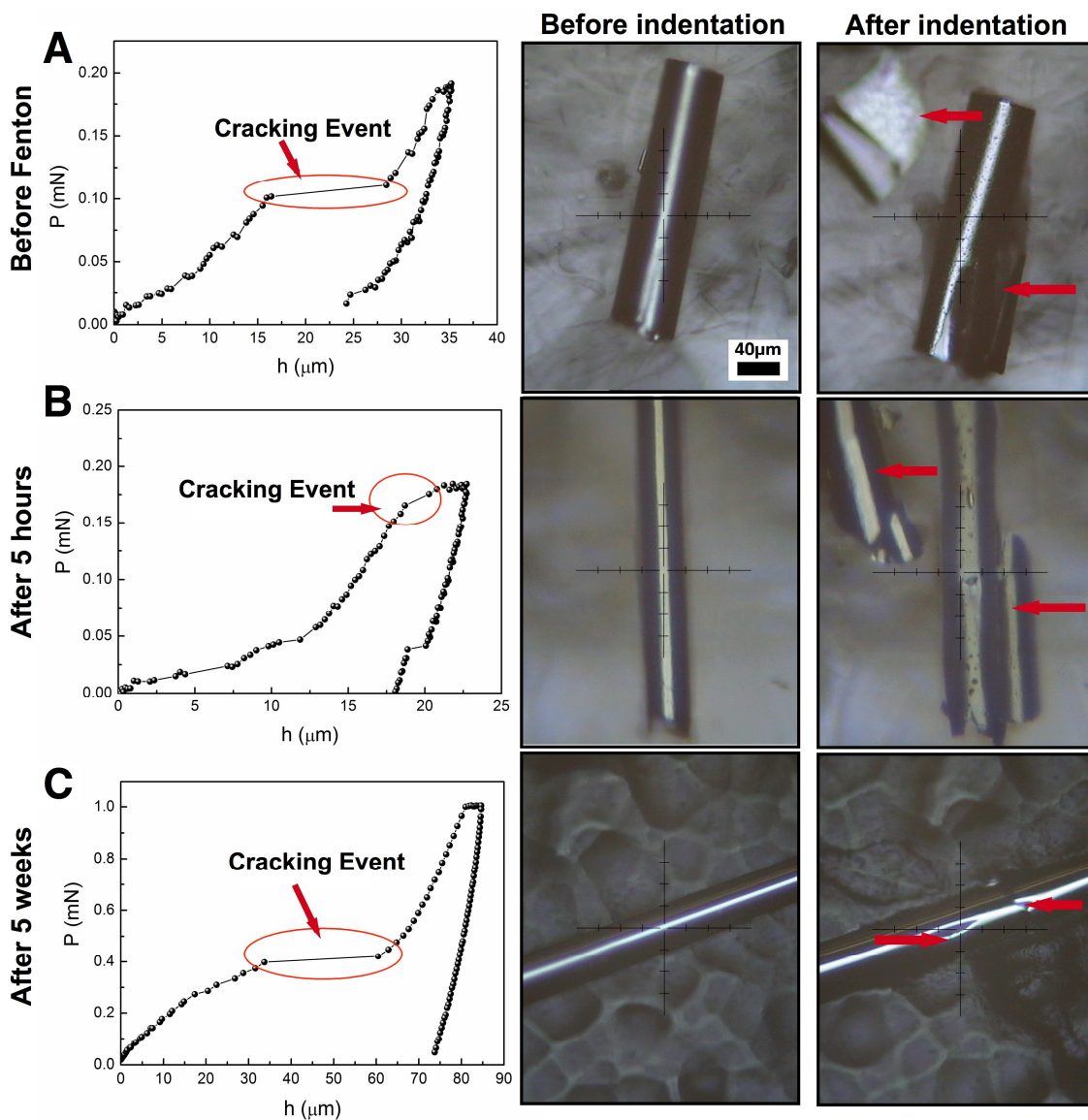
Figure 5. Representative load (P) – displacement (h) curves and optical microscopy images of micro-cleaners before indentation (center) and after indentation (right) corresponding to the micro-cleaners (A) before Fenton, (B) after 5 hours of Fenton and (C) after 5 weeks of storage. Arrows indicates chipped off layers and cracks of the micro-cleaners that occurred during indentation and, most likely, associated to the cracking event shown in the respective load-displacement curve.

Figure 5(A, left) shows the applied load (P) – penetration depth (h) indentation curve of a micro-cleaner before the Fenton reaction (i.e., an unused micro-cleaner). The test reveals a smooth loading behavior up to a load of about 0.1 mN, where a pronounced pop-in (i.e.,

sudden displacement burst) is observed. This displacement was associated to a cracking event of the material, and was further verified through optical microscopy. **Figure 5(A, center)** shows the image of the tubular micro-cleaner before indentation, while **Figure 5(B, right)** shows the same micro-cleaner after indentation. Arrows in **Figure 5(B, right)** indicates a layer of micro-cleaner that has been chipped away during indentation and, most likely, corresponds to the cracking event shown in **Figure 5(A, left).** A similar behavior, accompanied with a certain barreling of the micro-cleaners, was observed in all other investigated micro-cleaners before Fenton reaction.

A representative nanoindentation curve of the micro-cleaners after 5 hours of Fenton reaction is shown in **Figure 5(B, left).** The maximum penetration depth attained after Fenton reaction is smaller than before Fenton. Namely, h decreases from ~ 35 µm (before Fenton) to ~ 23 µm (after 5 hours), respectively. This means that the Fenton reaction induces an increase of the strength of the micro-cleaners. Cracking events and exfoliation of the micro-cleaners usually take place during indentation tests performed after Fenton reaction, although at loads typically close to 0.2 mN (see **Figures 5(B, center)** and **5(B, right)).** In summary, before Fenton reaction the micro-cleaners appear to be more ductile, with higher attained penetration depths than for micro-cleaners after Fenton reaction for a given value of maximum applied load (compare **Figures 5(A)** and **5(B)).** Both, before and after 5 hours of Fenton reaction, indentation tends to cause a certain barreling of the tubes (particularly before Fenton reaction) inducing, finally, cracking and exfoliation of the outer shells of the tubes. As aforementioned, after 5 hours of Fenton reaction micro-cleaners appear to be mechanically stiffer mainly because: (i) tightening up, reducing the diameter of the micro-cleaner and increasing the number of layers (i.e., their thickness) and (ii) the formation of iron oxides at the outer surface of the micro-cleaners as seen in the XPS analysis in **Figure 4(C)**.

Figure 5(C) shows the results of nanoindentation on a micro-cleaner after 5 weeks in storage. In this case, the penetration depth attained for an applied load of 0.2 mN is around 10 µm and no cracking events were observed for this maximum applied load. In order to assess whether exfoliation of the micro-cleaners takes place at higher loads, nanoindentation experiments were performed with P_{Max} = 1 mN. As it can be observed in **Figure 5(C, left)**, in this case a clear cracking event occurs at P ~ 0.6 mN. This critical load for cracking is therefore higher than the one observed in **Figures 5(A) and 5(B),** suggesting an increase of mechanical resistance of the micro-cleaners with usage. Typical optical microscopy images of these tubes before and after indentation with P_{Max} = 1 mN are shown in **Figures. 5(C, center)** and **5(C, right).**

Table 1. Summary of the elastic (U_{el}), plastic (U_{pl}) and total (U_{tot}) indentation energies for the micro-cleaners. The ratio U_{el}/U_{tot} corresponds to the elastic recovery of the indented micro-cleaners.

Tube	Elastic energy U_{el} (nJ)	Plastic energy U_{pl} (nJ)	Total energy U_{tot} (nJ)	U_{el}/U_{tot}
Before Fenton	0.97	2.71	3.68	0.26
After Fenton 5 hrs	0.46	1.83	2.29	0.20
After Fenton 5 weeks	2.13	1.67	3.80	0.56

Table 1 shows the energy analyses performed during indentation of the micro-cleaners for the three investigated conditions. Remarkably, the elastic recovery (i.e., the ratio between the elastic energy, U_{el}, and the total energy, U_{tot}) after 5 weeks of storage is clearly larger than before Fenton or after 5 hours of usage. Hence, from a mechanical point of view, the tubes after Fenton are better than before Fenton, as fracture is clearly delayed and the elastic

recovery is enhanced by more than a factor of 2 with respect to the as-prepared micro-cleaners before Fenton.
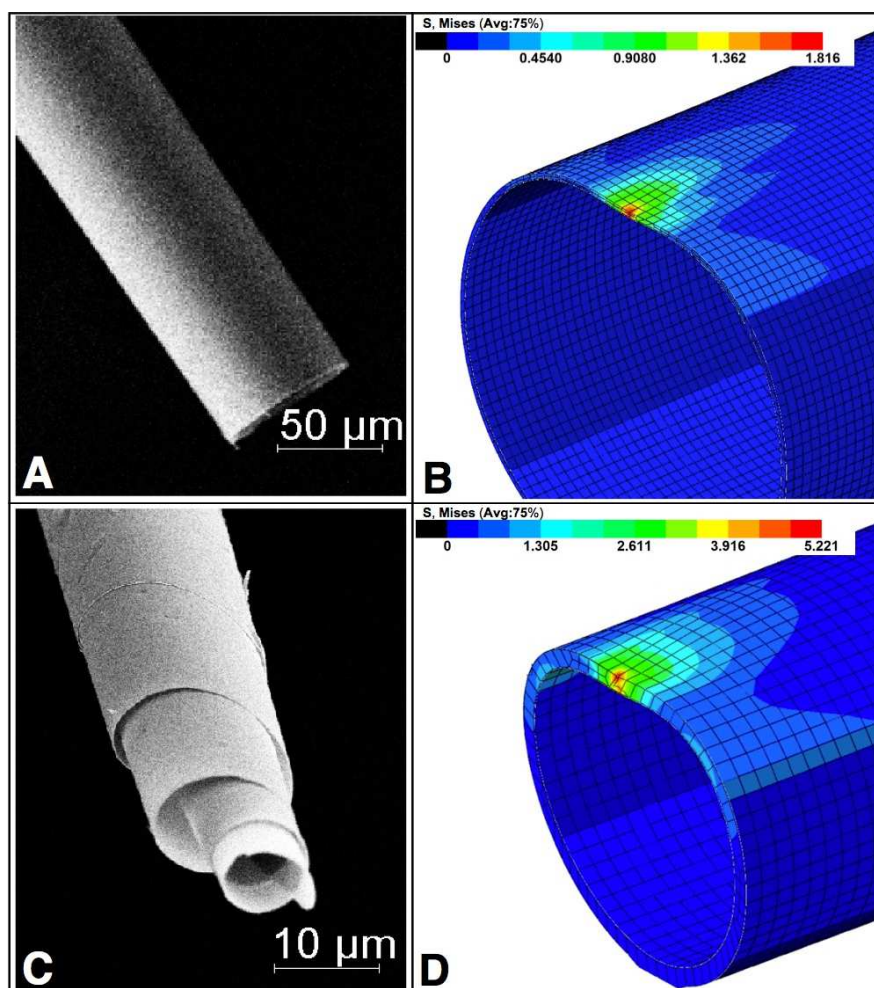

Figure 6. Scanning electron microscopy images and Finite Element Modelling of (A) a micro-cleaner before Fenton and (C) a micro-cleaner after Fenton reaction, together with the simulated von-Mises stress distribution of indented micro-cleaners with similar wall-to-thickness aspect ratios (B and D, respectively).

Additionally, nanoindentation finite element simulations were performed using the commercial software ABAQUS in order to shed further light on the mechanical performance of the micro-cleaners. The chosen geometry for the simulations was a cylinder with a wall-to-diameter aspect ratio similar to the investigated micro-cleaners before and after 5 hours of

Fenton reaction. The mesh used during the simulations consisted of fully-integrated brick-shape elements, Berkovich indenter was considered as a perfectly rigid body and the cylinders perfectly elastic, with a Young's modulus equal to 200 GPa. Boundary conditions were such as to prevent the vertical displacement of the cylinder during indentation. The von Mises yield criterion was used to study the differences in the mechanical performance of the micro-cleaners before and after 5 hours of Fenton reaction. The diameter of the micro clearers was decreased after the reaction (**Figure 6(A)** and **Figure 6(C))** due to the tightening of the layers, likely because of the pressure pulses generated during bubble development and release could promote the release of residual strains from the layers. The simulations reveal that the tube after Fenton reaction (**Figure 6(D))** accumulates higher stress directly beneath the indenter tip for a given applied load than the tube before Fenton reaction (**Figure 6(B)),** indicating that it is mechanically harder. Concomitantly, for a certain applied load, the overall deformation of the tube before Fenton reaction is higher than in the simulated tube after Fenton. The results of this simple simulation (which does not take into account the multiwall structure of the micro-tubes) agree qualitatively well with the experimental observations.

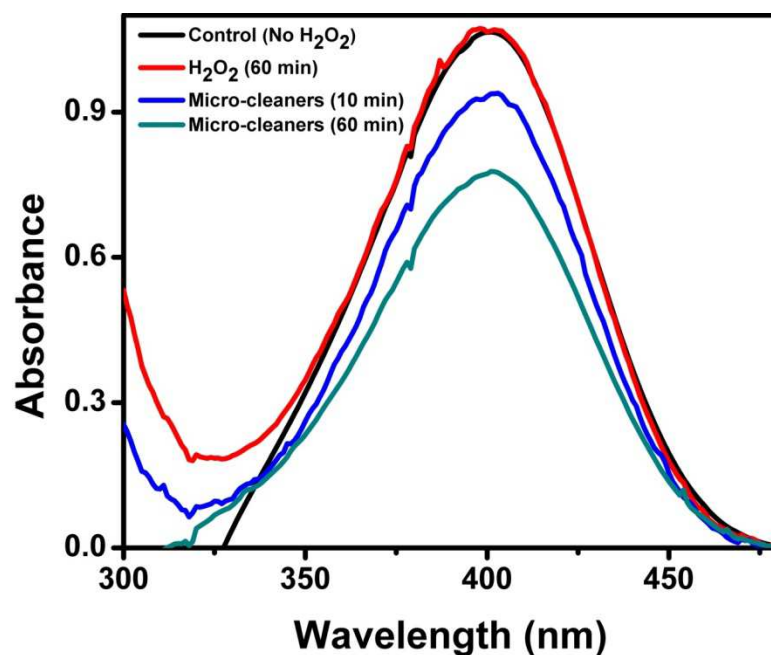**2.4 Degradation of phenolic compound**

Figure 7. Degradation of 4-nitrophenol by H_2O_2 control in 60 min. (red), 500µm micro-cleaners in 10 min. (blue) and 60 min. (cyan). Black lunes indicates control with H2O

In order to prove the remediation capabilities of micro-cleaners to other organic pollutants, we performed a degradation experiment for a phenolic compound (4-nitrophenol) using 500 µm micro-cleaners. 4-nitrophenol is one of the most common organic pollutant molecules present in the industrial wastewater. Its degradation is challenging using bacteria, yet hydroxyl radicals are capable of completely mineralizing it into carbon dioxide[57–59]. **Figure 7** shows that by using H_2O_2 as oxidant alone cannot degrade 4-nitrophenol, while micro-cleaners can degrade more than 30% in 60 minutes. The difference in the percentage of degradation for malachite green and 4-nitrophenol is due to the different reaction kinetics of hydroxyl radicals for different organic molecules. Micro-cleaners degraded ~18 µg of 4-nitrophenol in 10 minutes and ~41µg in 60 minutes from 3 mL of contaminated water containing 150 µg of initial amount (50µg/ml). Longer duration is required to achieve complete degradation but also the addition of larger amounts of micro-cleaners could achieve faster oxidation and even total degradation.

3. Conclusions

We demonstrated the reusability of self-propelled Fe/Pt micro-cleaners that can carry out highly active Fenton-like reaction without external mixing. We found that the variation in the length of micro-cleaners does not affect the performance if the amount of catalytic material that is rolled-up is kept constant. Reusability results showed that the micro-cleaners can be recovered using magnets and reused for multiple times within less than a week without the decrease in the performance of the organic degradation. Several weeks storage is possible without much sacrificing the activity. Micro-cleaners can also be used for continuous

21

swimming applications, namely at least 24 hours. We observed that the surface micro-cleaners were oxidized to produce *in situ* iron oxides which act as a heterogeneous catalyst. Iron oxides formation along with the tightening of rolled up layers increase the mechanical strength of the micro-cleaners after the Fenton reaction. Degradation experiments of 4-nitrophenol and malachite green proved the possibility of using micro-cleaners for wide range of organic pollutants. The experiments presented here, evidence the long-term and reusability of very active micro-cleaners, which will be beneficial towards lowering the cost of the water treatment using this advanced technology. Further experiments should be driven towards the remediation of other pollutants in real wastewater samples and in confined pipes or places difficult to reach by traditional methods.

Experimental section

Fabrication of the micro-cleaners

Micro-cleaners were fabricated by rolling up the nanomembranes of iron and platinum metal deposited on square patterns of photoresist. Positive photoresist patterns (200 μm, 300 μm and 500 μm) were developed using standard photolithography techniques. Positive photoresist (ARP 3510) was spin coated (3500 rpm for 35 s) on previously cleaned glass wafers (18x18mm) to make a layer with uniform thickness (2.4 μm) and exposed to the UV light under a chromium mask with the respective sizes of patterns confined in 1 cm^2 area by a mask aligner. Photolithographic patterns on glass substrates were developed (using 1:1 water/AR 300) and dried by blowing nitrogen before depositing the metal nanomembranes. A custom built e-beam evaporator was used for the deposition. Two layers of iron (100 nm) were evaporated at different deposition rates (at 0.30 nms^{-1} and 0.06 nms^{-1} respectively); third layer of platinum (5 nm) was evaporated (at 0.02 nms^{-1}). All three layers were deposited at the glancing angle (65°), which leads to a non-deposited window at each pattern. The photoresist

22

walls, adjacent to the non-deposited windows, remain exposed which was required for the controlled directional rolling of nanomembranes. A mixture of dimethyl sulfoxide (DMSO) and acetone (1:1) was used to etch photoresist selectively from the exposed wall. The nanomembranes were rolled up from the side of the exposed wall to the unexposed wall in the shape of tubular micro-cleaners (Supporting videos).

Size effect and reusability and 4-nitrophenol degradation experiments

Three different sizes of micro-cleaners (200 µm, 300 µm and 500 µm long with the diameter between 40-60 µm) were fabricated from the nanomembranes deposited on photoresist patterns that were confined in 1 cm^2 area on the glass substrate. The number of micro-cleaners rolled up from a constant amount of catalytic material present in 0.64 cm^2 area including all square patterns were different for different sizes of patterns (~1600, ~729, ~ 256 respectively for sizes in increasing order). After rolling up, micro-cleaners were first transferred into SDS water (0.5 % w/v) and then used for degradation experiments, carried out in a beaker containing total 3 ml of polluted water consisted of malachite green (50 µg/ml), hydrogen peroxide (15% v/v) and SDS (0.5 % w/v) at the adjusted acidic pH (2.5). Dye concentration was measured by a spectrophotometer (Specord 250, Analytical Jena) at 0, 10, 30 and 60 minutes during the experiments to study the effect of sizes. A new batch of 500 µm micro-cleaners was fabricated and used to study the effect of hydrogen peroxide concentration (5%, 10%, 15%, 20% and 25%) on the degradation of malachite green in 60 minutes. Degradation of 4-nitrophenol (50 µg/ml) was carried out by using 500 µm micro-cleaners in the same experimental condition used for malachite green degradation.

In a different batch, micro-cleaners of all sizes were fabricated using the same parameters that were used for size effect experiments to study the reusability. All three sizes of micro-cleaners were reused after short and long term storage. Short-term experiments were carried out at

varying time intervals; first five cycles were carried out at 1 to 5 hours continuously changing polluted water after the end of the 60 minutes of a degradation cycle. After the end of each cycle, micro-cleaners were confined in a corner of the beaker using a strong neodymium-iron-boron hard magnet and the treated water was replaced with pure water (Millipore water) to clean the surfaces of micro-cleaners, cleaning step is repeated twice and then polluted water solution is added for the next cycle. Polluted water composition was kept same as in the size effect experiments. After 5 hours, micro-cleaners were cleaned and stored in SDS water (0.5% w/v) before using in next cycles at 18 hours and 24 hours form the first cycle. In a similar fashion, long term storage experiments were carried out using the same micro-cleaners after 1 week of intermediate storage between two cycles up to 5 weeks from the first cycle. Dye concentration after each cycle was measured by the UV-Vis spectrophotometer. After each cycle, treated water was collected and further analyzed by ion coupled plasma (ICP-OES) method to measure the iron concentration that was leached from the surface of micro-cleaners.

Continuous swimming and video recording

An upright microscope (Leica DFC3000G camera) was used to record rolling up videos for different sizes of micro-cleaners (supporting videos) while an inverted microscope (Leica DMI300B) was used to study the swimming behavior of micro-cleaners after each cleaning cycle. A custom designed 3D printed microscope stage was fabricated to record the swimming of micro-cleaners directly in the beaker where the degradation experiment was going on.

During the continuous swimming experiment, micro-cleaners were observed under the inverted microscope at 1, 5 and 24 hours.

Surface characterization

X-ray photoelectron spectroscopy (XPS) analyses were carried out on a PHI 5500 Multitechnique System (from Physical Electronics) spectrometer, equipped with a monochromatic X-ray source ($K_{\alpha Al}$ line with energy of 1486.6 eV and 350 W), placed perpendicular to the analyser axis and calibrated using $3d^{5/2}$ line of Ag with a full width at half maximum (FWHM) of 0.8 eV. The analysed area was a 0.8 mm diameter disk surface for each sample. Charging effects were corrected by referencing the binding energies to that of the adventitious Cls line at 284.5 eV.

Mechanical properties

Micro-cleaners were dried using an ethanol-CO_2 critical point dryer before doing the nano-indentation experiments. Typical load-displacement measurements were conducted on the micro-cleaners before Fenton reaction, after 5 hrs of Fenton reaction and after 5 weeks. For the sake of simplicity, the micro-cleaners obtained from the 500 x 500 µm Fe/Pt layers were selected for the mechanical tests. Experiments were performed in load-control mode, using a UMIS instrument from Fischer-Cripps Laboratories equipped with a Berkovich pyramidal-shaped diamond tip. Maximum applied load values ranged between 0.2 mN and 1 mN. To ensure statistically meaningful results, at least 10 indentations were performed for each type of micro-cleaners and the representative average behaviour is reported. The elastic (U_{el}) and plastic (U_{pl}) energies during indentation were assessed from the areas enclosed between the unloading segment and displacement axis (U_{el}), and between the loading and unloading segments (U_{pl}). The total indentation energy is $U_{tot} = U_{el} + U_{pl}$ and corresponds to the area enclosed between the loading segment and the displacement axis. The ratio U_{el}/U_{tot} denotes to the elastic recovery of the tubes after having been indented.

Supporting Information

Supporting Information is available from the Wiley Online Library or from the author.

Received: ((will be filled in by the editorial staff))

Revised: ((will be filled in by the editorial staff))

Published online: ((will be filled in by the editorial staff))

[1]   D. W. Kolpin, E. T. Furlong, M. T. Meyer, E. M. Thurman, S. D. Zaugg, L. B. Barber, H. T. Buxton, *Environ. Sci. Technol.* **2002**, *36*, 1202.
[2]   P. E. Stackelberg, E. T. Furlong, M. T. Meyer, S. D. Zaugg, A. K. Henderson, D. B. Reissman, *Sci. Total Environ.* **2004**, *329*, 99.
[3]   K. Fent, A. A. Weston, D. Caminada, *Aquat. Toxicol.* **2006**, *76*, 122.
[4]   P. R. Gogate, A. B. Pandit, *Adv. Environ. Res.* **2004**, *8*, 501.
[5]   P. C. Vandevivere, R. Bianchi, W. Verstraete, *J. Chem. Technol. Biotechnol.* **1998**, *72*, 289.
[6]   T. Robinson, G. McMullan, R. Marchant, P. Nigam, *Bioresour. Technol.* **2001**, *77*, 247.
[7]   T. A. Ternes, M. Meisenheimer, D. McDowell, F. Sacher, H.-J. Brauch, B. Haist-Gulde, G. Preuss, U. Wilme, N. Zulei-Seibert, *Environ. Sci. Technol.* **2002**, *36*, 3855.
[8]   M. Klavarioti, D. Mantzavinos, D. Kassinos, *Environ. Int.* **2009**, *35*, 402.

[9] D. Garrick, J. W. Hall, *Annu. Rev. Environ. Resour.* **2014**, *39*, 611.

[10] M. Falkenmark, *Philos. Trans. R. Soc. Lond. Math. Phys. Eng. Sci.* **2013**, *371*, 20120410.

[11] T. I. Veldkamp, Y. Wada, H. de Moel, M. Kummu, S. Eisner, J. C. Aerts, P. J. Ward, *Glob. Environ. Change* **2015**, *32*, 18.

[12] X. Qu, P. J. Alvarez, Q. Li, *Water Res.* **2013**, *47*, 3931.

[13] M. A. Shannon, P. W. Bohn, M. Elimelech, J. G. Georgiadis, B. J. Marinas, A. M. Mayes, *Nature* **2008**, *452*, 301.

[14] F. Perreault, A. F. de Faria, M. Elimelech, *Chem. Soc. Rev.* **2015**.

[15] S. Sánchez, L. Soler, J. Katuri, *Angew. Chem. Int. Ed.* **2015**, *54*, 1414.

[16] H. Wang, M. Pumera, *Chem. Rev.* **2015**, *115*, 8704.

[17] J. Wang, *Nanomachines: fundamentals and applications*; John Wiley & Sons, 2013.

[18] W. Duan, W. Wang, S. Das, V. Yadav, T. E. Mallouk, A. Sen, *Annu. Rev. Anal. Chem.* **2015**, *8*, 311.

[19] V. V. Singh, F. Soto, K. Kaufmann, J. Wang, *Angew. Chem.* **2015**.

[20] J. G. S. Moo, H. Wang, M. Pumera, *Chem. Commun.* **2014**, *50*, 15849.

[21] M. Guix, C. C. Mayorga-Martinez, A. Merkoçi, *Chem. Rev.* **2014**, *114*, 6285.

[22] J. Wang, W. Gao, *ACS Nano* **2012**, *6*, 5745.

[23] K. K. Dey, F. Wong, A. Altemose, A. Sen, *Curr. Opin. Colloid Interface Sci.* doi:10.1016/j.cocis.2015.12.001

[24] L. Soler, S. Sánchez, *Nanoscale* **2014**, *6*, 7175.

[25] W. Gao, J. Wang, *Acs Nano* **2014**, *8*, 3170.

[26] L. Soler, V. Magdanz, V. M. Fomin, S. Sanchez, O. G. Schmidt, *ACS Nano* **2013**, *7*, 9611.

[27] T. Li, L. Li, W. Song, L. Wang, G. Shao, G. Zhang, *ECS J. Solid State Sci. Technol.* **2015**, *4*, S3016.

[28] O. M. Wani, M. Safdar, N. Kinnunen, J. Jänis, *Chem. Eur. J.* **2015**.

[29] S. K. Srivastava, M. Guix, O. G. Schmidt, *Nano Lett.* **2016**, *16*, 817.

[30] J. Orozco, G. Cheng, D. Vilela, S. Sattayasamitsathit, R. Vazquez-Duhalt, G. Valdés-Ramírez, O. S. Pak, A. Escarpa, C. Kan, J. Wang, *Angew. Chem. Int. Ed.* **2013**, *52*, 13276.

[31] J. Li, V. V. Singh, S. Sattayasamitsathit, J. Orozco, K. Kaufmann, R. Dong, W. Gao, B. Jurado-Sanchez, Y. Fedorak, J. Wang, *ACS Nano* **2014**, *8*, 11118.

[32] V. V. Singh, J. Wang, *Nanoscale* **2015**, *7*, 19377.

[33] J. G. S. Moo, H. Wang, G. Zhao, M. Pumera, *Chem.- Eur. J.* **2014**, *20*, 4292.

[34] M. Xuan, X. Lin, J. Shao, L. Dai, Q. He, *ChemPhysChem* **2015**, *16*, 147.

[35] M. Guix, J. Orozco, M. García, W. Gao, S. Sattayasamitsathit, A. Merkoçi, A. Escarpa, J. Wang, *ACS Nano* **2012**, *6*, 4445.

[36] E. Brillas, I. Sirés, M. A. Oturan, *Chem. Rev.* **2009**, *109*, 6570.

[37] A. Goti, F. Cardona, In *Green Chemical Reactions*; Tundo, P.; Esposito, V., Eds.; NATO Science for Peace and Security Series; Springer Netherlands, 2008; pp. 191–212.

[38] R. Noyori, M. Aoki, K. Sato, *Chem. Commun.* **2003**, 1977.

[39] E. Neyens, J. Baeyens, *J. Hazard. Mater.* **2003**, *98*, 33.

[40] I. Oller, S. Malato, J. Sánchez-Pérez, *Sci. Total Environ.* **2011**, *409*, 4141.

[41] A. D. Bokare, W. Choi, *J. Hazard. Mater.* **6**, *275*, 121.

[42] A. Babuponnusami, K. Muthukumar, *J. Environ. Chem. Eng.* **2014**, *2*, 557.

[43] M. Pereira, L. Oliveira, E. Murad, *Clay Miner.* **2012**, *47*, 285.

[44] B. H. Hameed, T. W. Lee, *J. Hazard. Mater.* **2009**, *164*, 468.

[45] V. M. Fomin, M. Hippler, V. Magdanz, L. Soler, S. Sanchez, O. G. Schmidt, *IEEE Trans. Robot.* **2014**, *30*, 40.

[46] L. Li, J. Wang, T. Li, W. Song, G. Zhang, *J. Appl. Phys.* **2015**, *117*, 104308.

[47]   J. Orozco, B. Jurado-Sánchez, G. Wagner, W. Gao, R. Vazquez-Duhalt, S. Sattayasamitsathit, M. Galarnyk, A. Cortés, D. Saintillan, J. Wang, *Langmuir* **2014**, *30*, 5082.

[48]   C. Hsueh, Y. Huang, C. Wang, C.-Y. Chen, *Chemosphere* **2005**, *58*, 1409.

[49]   L. Gomathi Devi, S. Girish Kumar, K. Mohan Reddy, C. Munikrishnappa, *J. Hazard. Mater.* **2009**, *164*, 459.

[50]   M. A. Oturan, E. Guivarch, N. Oturan, I. Sirés, *Appl. Catal. B Environ.* **2008**, *82*, 244.

[51]   I. S. Khalil, V. Magdanz, S. Sanchez, O. G. Schmidt, S. Misra, E. Ben-Jacob, *PloS One* **2014**, *9*, e83053.

[52]   J. R. Scheffe, A. Francés, D. M. King, X. Liang, B. A. Branch, A. S. Cavanagh, S. M. George, A. W. Weimer, *Thin Solid Films* **2009**, *517*, 1874.

[53]   N. Srivastava, T. Shripathi, P. C. Srivastava, *J. Electron Spectrosc. Relat. Phenom.* **2013**, *191*, 20.

[54]   M. Descostes, F. Mercier, N. Thromat, C. Beaucaire, M. Gautier-Soyer, *Appl. Surf. Sci.* **2000**, *165*, 288.

[55]   Y.-D. Luo, Y.-H. Lin, X. Zhang, D. Liu, Y. Shen, C.-W. Nan, Y.-D. Luo, Y.-H. Lin, X. Zhang, D. Liu, Y. Shen, C.-W. Nan, *J. Nanomater. J. Nanomater.* **2013**, *2013, 2013*, e252593.

[56]   G. Cabello, A. Araneda, L. Lillo, C. Caro, C. Venegas, M. Tejos, B. Chornik, *Solid State Sci.* **2014**, *27*, 24.

[57]   M. A. Oturan, J. Peiroten, P. Chartrin, A. J. Acher, *Environ. Sci. Technol.* **2000**, *34*, 3474.

[58]   M. Kuosa, J. Kallas, A. Häkkinen, *J. Environ. Chem. Eng.* **2015**, *3*, 325.

[59]   S.-P. Sun, A. T. Lemley, *J. Mol. Catal. Chem.* **2011**, *349*, 71.